Laser-noise-induced population fluctuations in two-level systems: Complex and real Gaussian driving fields

R. Walser and H. Ritsch
Institut für Theoretische Physik, Universität Innsbruck, A-6020 Innsbruck, Austria
and Joint Institute for Laboratory Astrophysics, University of Colorado, Boulder, Colorado 80309-0440

P. Zoller and J. Cooper
Joint Institute for Laboratory Astrophysics, University of Colorado, Boulder, Colorado 80309-0440
(Received 12 August 1991)

The nonlinear dynamics of a sample of two-level systems exposed to noisy laser light is investigated. As stochastic models we treat the chaotic field and the real Gaussian field. Based on the method of marginal characteristic functions, we deduce analytical solutions for the mean values and variances of the atomic populations in terms of matrix continued fractions. We find significantly enhanced on-resonance fluctuations for a real Gaussian field compared to a chaotic field of the same bandwidth and intensity. Furthermore, in contrast to phase-noise models, the fluctuations in the fluorescence intensity do not decrease to zero in the limit of slow fluctuations.

PACS number(s): 42.50.Lc, 32.50.+d, 32.80.−t

I. INTRODUCTION

In a series of recent publications it has been demonstrated theoretically [1–5] and experimentally [6–8] that the relatively large intensity fluctuations in the resonance fluorescence of a macroscopic sample of atoms can be attributed to laser noise. An analysis of the amount and frequency distribution of these fluctuations has revealed much more detailed information about the input field fluctuations that can be obtained by simply looking at the mean values of the fluorescence intensity. In particular, fields with an identical spectrum can lead to qualitatively different fluctuation behavior, exhibiting the differences in higher-order field-correlation functions. On the other hand, these fluctuations very often limit the accuracy and speed of optical high-precision experiments, so that understanding the precise origin of this detrimental noise could also help to improve such experiments.

Apart from calculations using lowest-order perturbation theory, most of the work in this field has concentrated on phase-noise models such as the phase-diffusion model (PDM) and the phase-jump model [1]. These noise fields model stabilized single-mode lasers. In this work we will focus on models exhibiting mainly amplitude noise, such as the real Gaussian field and the complex Gaussian field, which contain amplitude and phase fluctuations. While the complex Gaussian field emerges naturally as a well-suited approximation to the output of a freely running multimode laser or even to thermal light emerging from a light bulb, there is no such obvious natural source for a real Gaussian field. However, there have been a series of recent experimental demonstrations of the generation and application of such a real Gaussian field by Elliott and co-workers [7,9] with well-defined and controlled properties.

This paper is organized as follows. In Sec. II we have compiled the basic equations necessary for describing the atomic system as well as the fundamental features of the stochastic light models under consideration. Section III presents a short outline of the method used to solve the stochastic atom-field interactions for a complex and real Gaussian field. The results for the mean emitted fluorescence intensity and its variance are discussed in Sec. IV for the two considered light models. In addition, we compare our results with the corresponding predictions for a phase-jump and a phase-diffusion model.

II. BASIC EQUATIONS

A. Atomic quantities

1. Photodetection of atomic fluorescence

Following the standard approach to the theory of photodetection [10], one finds that the mean photocurrent for a photodetector at position $\mathbf{x}$, with a surface A and a dimensionless quantum efficiency η, is given by

$$\langle\langle i(t)\rangle\rangle = \eta \int_A d^2x \langle\langle \langle :I(\mathbf{x},t):\rangle \rangle\rangle \ . \tag{1}$$

Here $\langle\langle\ \rangle\rangle$ is the abbreviation for stochastic averaging and $\langle :I(\mathbf{x},t):\rangle$ denotes the normally ordered quantum expectation value for the intensity operator. We assume our sample consists of many (N) independent atoms exposed to the same fluctuating laser field. In order to connect the mean intensity to the intensity contributions of the individual atoms in a simple way, we have to neglect any cooperative effects. Assuming all necessary restrictions [2] means that the mean intensity is just the sum over the intensity contributions from all atoms

$$I(\mathbf{x},t) = \sum_{k=1}^{N} I^{(k)}(\mathbf{x},t) \ , \tag{2}$$

and the mean photocurrent is given by

$$\langle\langle i(t)\rangle\rangle = \eta N \kappa \frac{\Omega_A}{4\pi} \left\langle\left\langle \rho_{11}\left(t-\frac{r}{c}\right)\right\rangle\right\rangle . \tag{3}$$

Here Ω_A is the fraction of the emitted fluorescence intensity that is collected by the detector, while κ denotes the inverse lifetime of the excited state. The central observable we are interested in here is the symmetric two-time photocurrent correlation function, which under the above assumptions is given by

$$\langle\langle i(t)i(t+\tau)\rangle\rangle = \left[\eta N \kappa \frac{\Omega_A}{4\pi}\right]^2 \langle\langle \rho_{11}(t)\rho_{11}(t+\tau)\rangle\rangle . \tag{4}$$

The corresponding spectrum $S(\nu)$ is

$$S(\nu) = 2\int_0^\infty \cos(\nu\tau)\langle\langle i(t), i(t+\tau)\rangle\rangle d\tau . \tag{5}$$

Here we have adopted the notation

$$\langle\langle i(t), i(t+\tau)\rangle\rangle = \langle\langle i(t)i(t+\tau)\rangle\rangle - \langle\langle i(t)\rangle\rangle\langle\langle i(t+\tau)\rangle\rangle .$$

The standard deviation for the intensity fluctuations is defined as the integrated spectrum

$$\Delta(i(t)) = \sqrt{\langle\langle i(t), i(t)\rangle\rangle} = \left[\int_{-\infty}^{\infty} d\omega\, S(\omega)\right]^{1/2} .$$

2. *Atomic time evolution*

Within the standard approximations of quantum optics [11], it is possible to deduce an equation of motion for the density operator $\underline{\rho}_A(t)$ of an atom coupled to a stochastic electromagnetic field. We will restrict ourselves to the case of a two-level atom (TLA), which leads to the following set of stochastic Bloch equations for the four components of $\underline{\rho}_A(t)$:

$$\left[\frac{d}{dt} - \begin{pmatrix} z & 0 & i\frac{\Omega(t)}{2}e^{i\varphi(t)} & 0 \\ 0 & z^* & -i\frac{\Omega(t)}{2}e^{-i\varphi(t)} & 0 \\ i\Omega(t)e^{-i\varphi(t)} & -i\Omega(t)e^{i\varphi(t)} & -\kappa & -\kappa \\ 0 & 0 & 0 & 0 \end{pmatrix}\right] \begin{pmatrix} \overline{\rho_{01}} \\ \overline{\rho_{10}} \\ w \\ \mathrm{tr} \end{pmatrix} = 0 . \tag{6}$$

In Eq. (6) we have set $\overline{\rho_{01}}(t) = \rho_{01}e^{-i\omega t}$, $w(t) = \rho_{11}(t) - \rho_{00}(t)$, and $\mathrm{tr}(t) = \rho_{11} + \rho_{00} \equiv 1$; $\Omega(t) = 2\boldsymbol{\mu}\cdot\boldsymbol{\varepsilon}|\epsilon(t)|$ denotes the atomic Rabi frequency, with $\epsilon(t)e^{-i\omega t} = |\epsilon(t)|e^{-i\varphi(t)-i\omega t}$ the positive-frequency part of the stochastic c-number input field. Furthermore, we set $z = -i\delta - \kappa/2$, with $\delta = \omega - \omega_{10}$ the detuning between the atomic transition frequency and the mean optical frequency of the input field, and κ the inverse lifetime of the atomic upper state. To simplify the notation we will drop the overbar in the following.

It is obvious from Eq. (4) that in order to calculate the variance and the corresponding autocorrelation functions, we have to deal with equations for the squared atomic density matrix elements,

$$\left[\frac{d}{dt} - \begin{pmatrix} 2z & 0 & i\Omega e^{i\varphi} & 0 & 0 & 0 \\ 0 & 2z^* & 0 & -i\Omega e^{-i\varphi} & 0 & 0 \\ i\Omega e^{-i\varphi} & 0 & z-\kappa & 0 & -i\Omega e^{i\varphi} & \frac{i}{2}\Omega e^{i\varphi} \\ 0 & -i\Omega e^{i\varphi} & 0 & z^*-\kappa & i\Omega e^{-i\varphi} & -\frac{i}{2}\Omega e^{-i\varphi} \\ 0 & 0 & -\frac{i}{2}\Omega e^{-i\varphi} & \frac{i}{2}\Omega e^{i\varphi} & z+z^* & 0 \\ 0 & 0 & 2i\Omega e^{-i\varphi} & -2i\Omega e^{i\varphi} & 0 & -2\kappa \end{pmatrix}\right] \begin{pmatrix} \rho_{01}^2 \\ \rho_{10}^2 \\ \rho_{01}w \\ \rho_{10}w \\ \rho_{01}\rho_{10} \\ w^2 \end{pmatrix} = \begin{pmatrix} 0 \\ 0 \\ -\kappa\rho_{01} \\ -\kappa\rho_{10} \\ 0 \\ -2\kappa w \end{pmatrix} , \tag{7}$$

where we have suppressed the explicit time dependence of Ω and φ. To find an equation for the stochastic averages of the variables defined by this set of multiplicative stochastic differential equations it is necessary to specify the stochastic noise models of the driving fields.

B. Models for the stochastic input fields

The stochastic electric-field amplitude of the laser at the position of the atom with polarization $\boldsymbol{\varepsilon}$ can be written as

$$\mathbf{E}_{cl}^{(+)}(t) = e^{-i\omega t}\boldsymbol{\varepsilon}\epsilon(t) . \tag{8}$$

In this paper we will consider two light models, namely the real Gaussian field and the complex Gaussian field. A real Gaussian field is defined by a real amplitude $\epsilon(t)$, which obeys an Ornstein-Uhlenbeck process [12]. In the complex Gaussian field the two quadrature components are assumed to obey two independent Ornstein-Uhlenbck processes [13]. Both models are characterized by a Lorentzian laser spectrum. We will denote the bandwidth of these fields by b and the mean intensity by

$\langle\langle \epsilon\epsilon^* \rangle\rangle$ ($\langle\langle \epsilon^2 \rangle\rangle$). Although both models have the same autocorrelation function they differ in their higher-order statistics. For comparison, the PDM and the phase-jump model considered in our previous work [1,2] describe pure phase fluctuations.

1. The chaotic field

It is well known [14] that the electric field of a multimode laser $\epsilon(t)=\sum_i \epsilon_i e^{-i\phi_i - i\omega_i t}$ obeys Gaussian statistics if the phases of the individual modes can be assumed independent,

$$P(|\epsilon|)=\frac{1}{\pi\langle\langle \epsilon\epsilon^* \rangle\rangle} e^{-(\epsilon\epsilon^*/\langle\langle \epsilon\epsilon^* \rangle\rangle)} . \tag{9}$$

Thus a multimode laser with a larger number of modes is well described by a chaotic field. It is therefore completely characterized by its first-order correlation function $\langle\langle \epsilon^*(t_1)\epsilon(t_2) \rangle\rangle$ ($\equiv$autocorrelation function).

A complex Gaussian (chaotic) field $\epsilon(t)=x(t)+iy(t)$ with Lorentzian spectrum and bandwidth b^c can be written as a solution of the Langevin equations

$$\begin{aligned} \frac{d}{dt}x &= -b^c x(t)+(b^c\langle\langle \epsilon\epsilon^* \rangle\rangle)^{1/2}F_1(t) , \\ \frac{d}{dt}y &= -b^c y(t)+(b^c\langle\langle \epsilon\epsilon^* \rangle\rangle)^{1/2}F_2(t) , \end{aligned} \tag{10}$$

with Gaussian random forces obeying $\langle\langle F_i(t)F_j(\bar{t}) \rangle\rangle = \delta_{ij}\delta(t-\bar{t})$ and $\langle\langle F_i(t) \rangle\rangle = 0$. The average of the moments of the incident intensity $I=\epsilon\epsilon^*$ are

$$\langle\langle I^n \rangle\rangle = n!\langle\langle \epsilon\epsilon^* \rangle\rangle^n , \tag{11}$$

and the relative intensity fluctuations are $\Delta I/\langle\langle I \rangle\rangle = 1$.

2. The real Gaussian field

The real Gaussian field can be viewed as the limit of a two-dimensional Markov process where the noise in one quadrature component is strongly suppressed. This is the classical analog of a squeezed vacuum: one has strong fluctuations in one quadrature component and no fluctuations in the other. However, in contrast to squeezing, all field-correlation functions stay positive in this case. In this limit the Langevin equation for the real field amplitude is

$$\frac{d}{dt}\epsilon = -b^r\epsilon(t)+(2b^r\langle\langle \epsilon^2 \rangle\rangle)^{1/2}F(t) , \tag{12}$$

with $\langle\langle F(t)F(\bar{t}) \rangle\rangle = \delta(t-\bar{t})$ and $\langle\langle F(t) \rangle\rangle = 0$. The stationary solution of the equivalent Fokker-Planck equation for the probability distribution of the amplitude is

$$P(\epsilon)=\frac{1}{(2\pi\langle\langle \epsilon^2 \rangle\rangle)^{1/2}} e^{-(\epsilon^2/2\langle\langle \epsilon^2 \rangle\rangle)} , \tag{13}$$

and the moments of the intensity $I=\epsilon^2$ are given by

$$\langle\langle I^n \rangle\rangle = (2n-1)!!\langle\langle \epsilon^2 \rangle\rangle^n , \tag{14}$$

with $(2n-1)!!=1\times3\times5\times\cdots\times(2n+1)$, and $(-1)!!=1$. Comparing this to the chaotic field, we see that the fluctuations for the real Gaussian field increase by a factor of $\sqrt{2}$, yielding $\Delta I/\langle\langle I \rangle\rangle = \sqrt{2}$.

III. ANALYTICAL SOLUTION FOR THE STOCHASTIC AVERAGES

In this section we will briefly outline a method of deriving analytical solutions for the averages and variances of the density matrix elements for the stochastic differential equations, Eqs. (6) and (7), for a real Gaussian and chaotic driving field. The method [14,15] is based on the fact that Eqs. (6) and (7) are multiplicative stochastic differential equations and that the driving field is Markovian. It has proven to be a powerful technique and has therefore been used in various calculations involving atoms driven by noise fields [16].

As a first step, we introduce the so-called *marginal characteristic functions*. With an appropriate Taylor ansatz the resulting partial differential equation is transformed into a difference-differential equation. Its stationary solution then can be found in the form of a matrix continued fraction. We will now demonstrate this method in more detail for the real Gaussian field.

A. The real Gaussian field

The Bloch equation [Eq. (6)] for the real Gaussian field has the form of

$$\frac{d}{dt}\mathbf{u}=[\underline{A}+\epsilon(t)\underline{B}]\mathbf{u}(t) , \tag{15}$$

with $\underline{A}$ and $\underline{B}$ as matrices and $\mathbf{u}$ as the vector of density matrix elements. By combining this equation with the Langevin equation for the driving field, we arrive at the following set of Langevin equations for the atom and field variables:

$$\frac{d}{dt}\begin{bmatrix}\mathbf{u}\\ \epsilon\end{bmatrix}=\begin{bmatrix}[\underline{A}+\epsilon(t)\underline{B}]\mathbf{u}(t)\\ -b\epsilon(t)\end{bmatrix}+\begin{bmatrix}0 & 0\\ 0 & \sqrt{2b}\end{bmatrix}\begin{bmatrix}0\\ F(t)\end{bmatrix} . \tag{16}$$

These equations define a Markov process [15,17], and the equivalent Fokker-Planck equation for the probability distribution $P(\mathbf{u},\epsilon,t)$ reads

$$\begin{aligned} \left[\frac{\partial}{\partial t}+L(\epsilon)\right]P(\mathbf{u},\epsilon,t) &= -\frac{\partial}{\partial\mathbf{u}}[(\underline{A}+\epsilon\underline{B})\mathbf{u}P(\mathbf{u},\epsilon,t)] , \\ L(\epsilon) &= -b\left[\frac{\partial}{\partial\epsilon}\epsilon+\langle\langle \epsilon^2 \rangle\rangle\frac{\partial^2}{\partial\epsilon^2}\right] . \end{aligned} \tag{17}$$

From Eq. (17) it is obvious that the equations for the atomic averages $\langle\langle \mathbf{u}(t) \rangle\rangle$ are coupled to equations for the combined atom-field averages $\langle\langle \mathbf{u}(t)\epsilon(t) \rangle\rangle$. These in turn are coupled to higher-order atom-field correlations, so that we end up with an infinite hierarchy of coupled equations. In order to treat this set of equations systematically we introduce marginal averages defined by

$$u_{\mu\nu}(\epsilon,t)=\int u_\mu u_\nu P(\mathbf{u},\epsilon,t)d^N u , \tag{18}$$

and their Fourier transforms, the characteristic marginal

averages

$$\tilde{u}_{\mu\nu}(\lambda,t)=\langle\langle u_\mu(t)e^{-i\lambda\epsilon(t)}u_\nu(t)\rangle\rangle$$
$$=\int e^{-i\lambda\epsilon}u_{\mu\nu}(\epsilon,t)d\epsilon\ . \tag{19}$$

The decorrelation of the atom-field averages [13] in the case of weak coupling between field and atoms ($\Omega_0 \ll \kappa, b, \delta$) suggests an ansatz in the following form:

$$\tilde{u}_{\mu\nu}(\lambda,t)=g_{\mu\nu}(\lambda,t)\langle\langle e^{-i\lambda\epsilon(t)}\rangle\rangle\ . \tag{20}$$

Consequently, we expect $g_{\mu\nu}(\lambda,t)$ to have a much smoother dependence on the parameter λ than $\tilde{u}(\lambda,t)$. Using Eq. (13), we can find

$$\langle\langle e^{-i\lambda\epsilon(t)}\rangle\rangle=e^{-\lambda^2/2}\ .$$

As a next step, we write a Taylor series for $g_{\mu\nu}(\lambda,t)$,

$$g_{\mu\nu}(\lambda,t)=\sum_{n=0}^{\infty}g^n_{\mu\nu}\lambda^n\ , \tag{21}$$

which, when inserted in Eq. (17) leads to the set of differential-difference equations:

$$\left[\frac{d}{dt}+bn\right]g^n_{\mu\nu}(t)=A_{\nu l}g^n_{l\mu}+A_{\mu l}g^n_{l\nu}$$
$$+i(n+1)(B_{\nu l}g^{n+1}_{l\mu}+B_{\mu l}g^{n+1}_{l\nu})$$
$$-i(B_{\nu l}g^{n-1}_{l\mu}+B_{\mu l}g^{n-1}_{l\nu})\ . \tag{22}$$

Introducing a vector $\mathbf{g}^n$

$$\mathbf{g}^n=(g^n_{11},g^n_{12},g^n_{13},g^n_{22},g^n_{23},g^n_{33},g^n_{41},g^n_{42},g^n_{43})^{\mathrm{T}}\ ,$$

and exploiting the symmetry of $g_{\mu\nu}$ and the matrices $\underline{A}$ and $\underline{B}$, we can rewrite Eq. (22) into a *tridiagonal vector recurrence relation* [15]

$$\left[\frac{d}{dt}+\underline{Q}_n\right]\mathbf{g}^n+\underline{Q}^{(-)}_n\mathbf{g}^{n-1}+\underline{Q}^{(+)}_n\mathbf{g}^{n+1}=\delta_{n,0}\mathbf{I}\ . \tag{23}$$

(The explicit expressions of the matrices can be found in Appendix A.) The stationary solution of Eq. (23) then can be given in terms of a matrix continued-fraction expansion

$$\mathbf{g}^0(\infty)=\lim_{t\to\infty}\mathbf{g}^0(t)=(\underline{Q}_0+\underline{Q}^{(+)}_0\underline{S}^{(+)}_0)^{-1}\mathbf{I}\ ,$$
$$\underline{S}^{(+)}_{n-1}=-(\underline{Q}_n+\underline{Q}^{(+)}_n\underline{S}^{(+)}_n)^{-1}\underline{Q}^{(-1)}_n\ . \tag{24}$$

In particular, we have

$$\langle\langle w^2\rangle\rangle=g^0_{33}(\infty),\quad \langle\langle w\rangle\rangle=g^0_{43}(\infty)\ , \tag{25}$$

which allows us to obtain easily all the relevant quantities of interest. In the case of fast fluctuations $b\gg\kappa,\Omega_0,\delta$ we can truncate Eq. (24) at $n=1$ to obtain explicit expressions for $\langle\langle w\rangle\rangle$ and $\langle\langle w^2\rangle\rangle$ as demonstrated in Appendix B. For the general case of arbitrary field-correlation time and strength, the continued-fraction solution to Eq. (24) can be evaluated numerically very efficiently and accurately.

B. The complex Gaussian field

Generalizing the above procedure to a chaotic field implies a Bloch equation of the form

$$\frac{d}{dt}\mathbf{u}=[\underline{A}+\epsilon(t)\underline{B}+\epsilon^*(t)\underline{C}]\mathbf{u}(t)\ . \tag{26}$$

To calculate the averages of the atomic variables it is again possible to transform Eq. (26) to an equivalent Fokker-Planck equation:

$$\left[\frac{\partial}{\partial t}+L(\epsilon,\epsilon^*)\right]P(\mathbf{u},\epsilon,t)$$
$$=-\frac{\partial}{\partial\mathbf{u}}\{[\underline{A}+\epsilon\underline{B}+\epsilon^*\underline{C}]\mathbf{u}P(\mathbf{u},\epsilon,t)\}\ ,$$
$$L(\epsilon,\epsilon^*)=-b\left[\frac{\partial}{\partial\epsilon}\epsilon+\frac{\partial}{\partial\epsilon^*}\epsilon^*+2\langle\langle\epsilon\epsilon^*\rangle\rangle\frac{\partial}{\partial\epsilon}\frac{\partial}{\partial\epsilon^*}\right]\ . \tag{27}$$

Proceeding analogously to the case of the real Gaussian field, we also introduce a marginal characteristic function. The main difference between the two cases arises from the fact that the stochastic process is now two dimensional. To obtain a simple one-dimensional recursion relation we have to write the Taylor series for the marginal characteristic averages

$$\langle\langle e^{-i\lambda\epsilon(t)-i\lambda^*\epsilon^*(t)}\rangle\rangle=e^{-\lambda\lambda^*}\ ,$$
$$\langle\langle w^2e^{-i\lambda\epsilon(t)-i\lambda^*\epsilon^*(t)}\rangle\rangle=e^{-\lambda\lambda^*}\sum_{n=0}^{\infty}g^n_{3,3}(t)\lambda^n\lambda^{*n}\ ,$$
$$\langle\langle\rho^2_{01}e^{-i\lambda\epsilon(t)-i\lambda^*\epsilon^*(t)}\rangle\rangle=e^{-\lambda\lambda^*}\sum_{n=0}^{\infty}g^n_{1,1}(t)\lambda^{n+2}\lambda^{*n}\ ,$$

etc. Making use of this ansatz, we again can derive a differential-difference equation analogous to Eq. (23), which again is solved by a matrix continued fraction (we have postponed the definitions of the coefficient matrices to Appendix A). Explicit expressions obtained by a first-order truncation of the continued fraction are presented in Appendix B.

IV. RESULTS AND DISCUSSION

In this section we discuss numerical results and analytical approximations for the mean values and variances of the atomic populations of an atom driven by real and complex Gaussian fields. In addition, we find it interesting to compare our predictions with our previous work [1], which considered an atomic system interacting with a phase-diffusing light field. In contrast to a real or complex Gaussian field, a phase-diffusing light field has no amplitude fluctuations. In comparing the atomic mean values and variances for these different field models, we assume that these light fields have the same mean intensity and bandwidth, i.e., have the same autocorrelation function but differ in the higher-order statistics.

In Figs. 1(a), 2(a), 3(a), and 4(a) we show the mean upper-state population $\langle\langle\rho_{11}\rangle\rangle$ as a function of the laser-atom detuning δ in units of κ. The corresponding variances $\Delta\rho_{11}$ are plotted in Figs. 1(b), 2(b), 3(b), and 4(b).

The dashed and solid lines correspond to the chaotic and real Gaussian fields, respectively, while the phase-diffusion results are plotted with dotted lines. In Figs. 1 and 2 we have chosen the bandwidth of the driving field to be smaller than the natural linewidth of the system, $b=0.25\kappa$, while the Rabi frequency

$$\Omega_0=[\langle\langle\,\Omega^*(t)\Omega(t)\,\rangle\rangle]_s^{1/2}$$

increases from weak fields to the limits of strong saturating fields, $\Omega_0=0.1\kappa$, 10κ. Figures 3 and 4 show our predictions for a broadband field, $b=5\kappa$, for the same Rabi frequencies.

One of the basic features apparent in these figures is that the averages of the upper-state population satisfy (PDM denotes phase-diffusion model; CGF and RGF denote complex and real Gaussian fields, respectively)

$$\langle\langle\rho_{11}\rangle\rangle_{\rm PDM}>\langle\langle\rho_{11}\rangle\rangle_{\rm CGF}>\langle\langle\rho_{11}\rangle\rangle_{\rm RGF}\,, \tag{28}$$

which reflects the different saturation behaviors of the stochastic fields. (For very low intensities, the atomic mean populations are identical because in this limit only the first-order correlation function enters, which is the same for all three models [Figs. 1(a) and 3(a)].) Similarly, we find for the variances (at least for a large range of detunings near resonance)

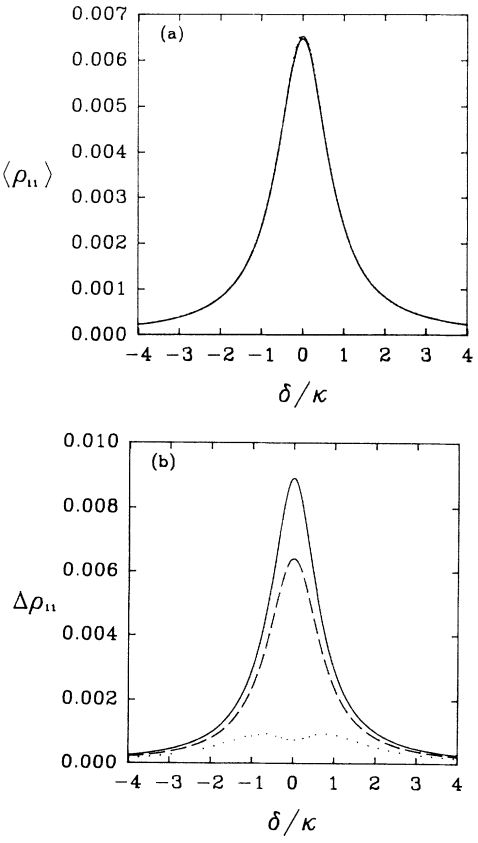

FIG. 1. (a) Mean population $\langle\langle\rho_{11}\rangle\rangle$ and (b) standard deviation $\Delta(\rho_{11})$ vs laser detuning δ/κ. The three curves represent the real Gaussian field (solid), chaotic Gaussian field (dashed), and phase-diffusion model [1] (dotted). The parameters are $\Omega_0=0.1\kappa$ and $b=0.25\kappa$.

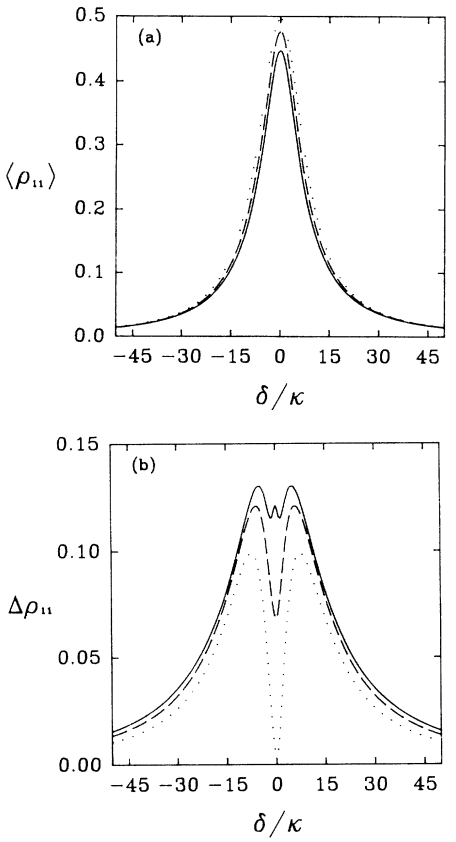

FIG. 2. Same as Fig. 1 with $\Omega_0=10\kappa$ and $b=0.25\kappa$.

$$(\Delta\rho_{11})_{\rm RGF}>(\Delta\rho_{11})_{\rm CGF}>(\Delta\rho_{11})_{\rm PDM}\,. \tag{29}$$

Qualitatively, this behavior is again related to the intensity fluctuations: for the chaotic field we have $\Delta I^2/\langle\langle I\rangle\rangle^2=1$, and $\Delta I^2/\langle\langle I\rangle\rangle^2=2$ for a real Gaussian field. The mean upper-state population [Figs. 1(a) and 2(a)] shows the usual resonance profiles with the width reflecting the natural linewidth, the spectral width of the field and the effects of power broadening with increasing intensity.

At low intensities and for small bandwidth $b<\kappa/2$, the laser-induced population fluctuations for the PDM show a minimum at resonance with two maxima at the points of maximum slope of the atomic population versus detuning [Fig. 1(b)] [1,8], while for large intensities we find a saturation dip [Fig. 2(b)]. In contrast, the real and complex Gaussian-field fluctuations are maximum on resonance in the weak-field limit [Fig. 1(b)], but again show a saturation hole for strong fields [Fig. 2(b)]. As an interesting new feature, the variance for the real Gaussian field exhibits a sharp narrow resonance of width $\approx\kappa/2$ superimposed on the broad background with width determined essentially by the Rabi frequency [Fig. 3(b)]. This feature is absent for the chaotic field. A physical interpretation of this peak will be given when we discuss the broadband limit.

The smaller the bandwidth of the field and the higher the intensity, the more terms are needed in the matrix continued-fraction expansion to achieve convergence.

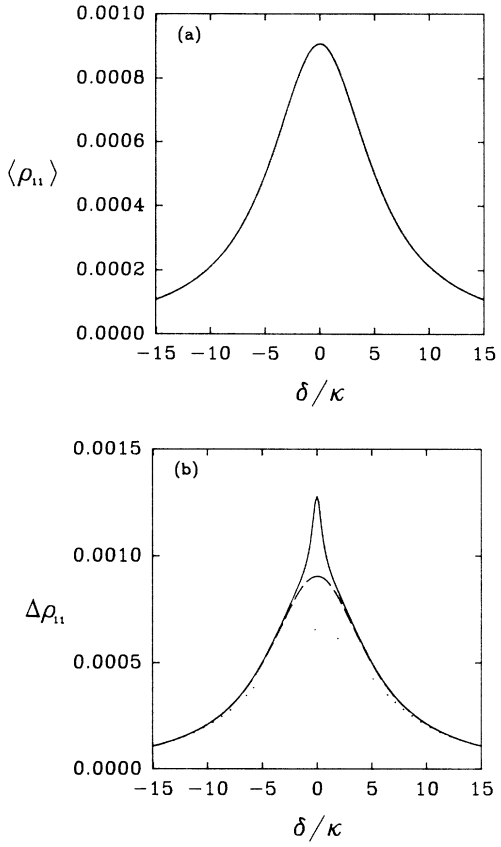

FIG. 3. Same as Fig. 1 with $\Omega_0=0.1\kappa$ and $b=5\kappa$.

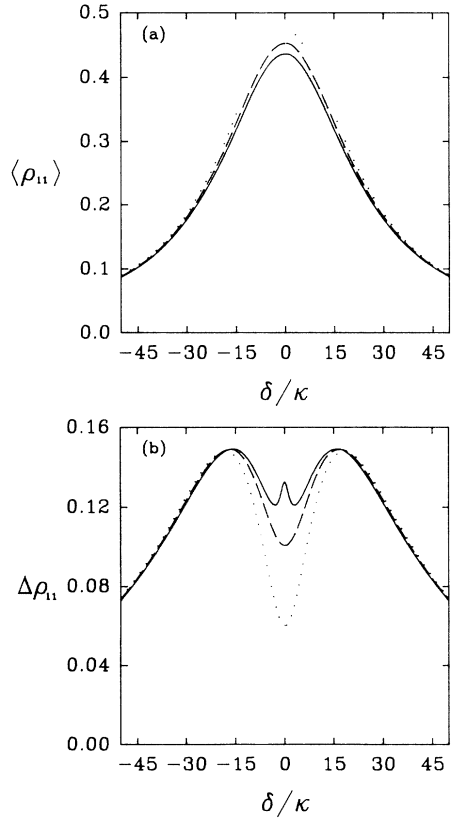

FIG. 4. Same as Fig. 1 with $\Omega_0=10\kappa$ and $b=5\kappa$.

The quasistatic limit $b\rightarrow 0$, on the other hand, can be solved quite easily by analytical methods. In this case the atomic variables are assumed to follow the driving-field fluctuations adiabatically. Derivations for the variances and mean population in the zero bandwidth limit can be found in Appendix C. We emphasize, however, that the narrow central peak in the variance of the real Gaussian field cannot be explained by this quasistatic approximation.

We turn now to a discussion of our results for broadband fields $b=5\kappa$ (Figs. 3 and 4); the other parameters are the same as in Figs. 1 and 2, respectively. The main difference for the mean upper-state population in Figs. 3(a) and 4(a) compared to Figs. 1(a) and 2(a) is a less effective saturation of the atomic transition accompanied by the expected broadening induced by the laser bandwidth. The standard deviations plotted in Figs. 3(b) and 4(b) look qualitatively similar to those found in the small-bandwidth case. The narrow feature for the real Gaussian field is similar to the one found in Fig. 2(b). In the present case the background is broader, while the central peak retains its width of $\approx\kappa/2$, independent of the laser bandwidth.

In the limit of broadband fields the matrix continued-fraction expansion can be truncated in low order. A discussion of the broadband limit and its relation to a white-noise approximation can be found in Appendix B. In this appendix, for detunings much less than the laser bandwidth, we derive the approximate relations

$$\left.\frac{\Delta\rho_{11}}{\langle\langle\rho_{11}\rangle\rangle}\right|_{\mathrm{CGF}}=\left[\frac{1}{1+2S}\right]^{1/2}, \tag{30}$$

with $S=\Omega^2/(\kappa b)$ the saturation parameter. The corresponding result for the real Gaussian field is

$$\left.\frac{\Delta\rho_{11}}{\langle\langle\rho_{11}\rangle\rangle}\right|_{\mathrm{RGF}}=\left[\frac{4(\delta/\kappa)^2+2(1+S)}{4(\delta/\kappa)^2(1+2S)+(1+S)(1+3S)}\right]^{1/2}, \tag{31}$$

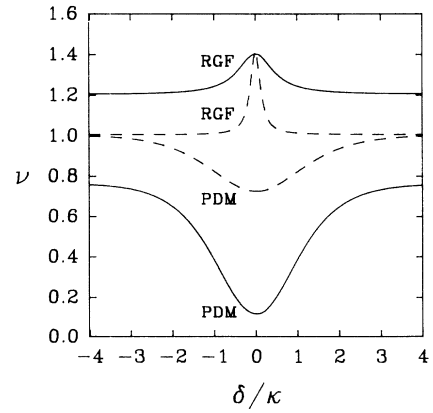

FIG. 5. The depicted curves show $\nu_{\mathrm{RGF(PDM)}}=(\Delta\rho_{11}/\langle\langle\rho_{11}\rangle\rangle|_{\mathrm{RGF(PDM)}})/(\Delta\rho_{11}/\langle\langle\rho_{11}\rangle\rangle|_{\mathrm{CFG}})$. The solid curve describes the same situation as in Fig. 1 $\Omega_0=0.1\kappa$, $b=0.25\kappa$, the dashed curve shows it for Fig. 3, $\Omega_0=0.1\kappa$, $b=5\kappa$.

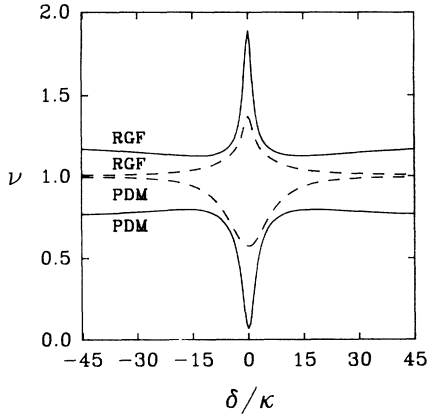

FIG. 6. Same as Fig. 2, but with $\Omega_0=10\kappa$, $b=0.25\kappa$ (solid line) and $\Omega_0=10\kappa$, $b=5\kappa$ (dashed line).

which shows the narrow resonance of width $\approx\kappa/2$. Physically speaking, this resonance structure in the real Gaussian field arises from the fact that a field with no phase fluctuations couples only to a specific quadrature component of the atomic polarization. The coupling of the driven atomic polarization component to the orthogonal polarization component arises only via the detuning. This uncoupled quadrature component is damped only by the natural decay rate but is, close to resonance, unaffected by the laser fluctuations. This leads to the narrow features in Figs. 2(b) and 4(b). In order to examine the statistics of the emitted radiation we have calculated the ratio

$$\nu=\frac{(\Delta\rho_{11}/\langle\langle\rho_{11}\rangle\rangle|_{\mathrm{RGF}})}{(\Delta\rho_{11}/\langle\langle\rho_{11}\rangle\rangle|_{\mathrm{CGF}})} .$$

We show this in Figs. 5 and 6.

V. CONCLUSIONS

In this paper we have studied the effects of laser noise on the fluorescence emitted by a large sample of two-level atoms. We have investigated the atomic mean populations and variance for the real and complex Gaussian fields of finite bandwidth. In comparison with the case of pure phase fluctuations [1], we find that for fields of the same mean intensity and bandwidth the presence of amplitude fluctuations significantly enhances and alters the dependence of the populations' variance on the laser and atomic parameters. For weak fields, the variance of the atomic population is determined by the fourth-order correlation function of the laser. Correspondingly, the real Gaussian field shows fluctuations larger than the complex Gaussian field, which again exhibits fluctuations much larger than for a field with pure phase noise. For strong fields we find that a saturation dip develops, which tends to suppress the noise near resonance. For the real Gaussian field we predict the appearance of a sharp resonance as a function of the population variance with width equal to the natural decay rate of the transition.

ACKNOWLEDGEMENTS

We thank M. H. Anderson, D. S. Elliott, and Gautam Vermuri for discussions and their interest. Work at JILA is supported by the National Science Foundation. H.R. was supported by the Austrian Fonds zur Förderung der wissenschaftlichen Forschung under Grant No. 7295. R.W. is grateful for support from the Austrian Bundesministerium für Wissenschaft und Forschung.

APPENDIX A: COEFFICIENT MATRICES

To complete the outline of our calculation we present the explicit definitions of the coefficient matrices cited in text [Eq. (23)].

In the chaotic field

$$\underline{Q}_n^{(+)}=\frac{\Omega}{2}(n+1)\underline{F} ,$$

with $F_{1,3}=F_{5,2}=2$, $F_{3,2}=F_{4,5}=-2$, $F_{3,6}=F_{7,9}=1$, and $F_{5,6}=F_{8,9}=-1$;

$$\underline{Q}_n^{(-)}=-\frac{\Omega}{2}\underline{G} ,$$

with $G_{2,3}=-1$, $G_{2,5}=1$, $G_{3,1}=G_{9,7}=2$, $G_{5,4}=G_{9,8}=-2$, $G_{6,3}=4$, and $G_{6,5}=-4$;

$$\mathbf{I}=-\kappa\mathbf{e}_9\delta_{n,0} ,$$

$$\underline{Q}_n=2bn\underline{1}_9-\frac{\Omega}{2}\underline{F}+\frac{\Omega}{2}n\underline{G}+\underline{H} ,$$

$$z=-i\delta-\frac{\kappa}{2} ,$$

with $H_{1,1}=H_{4,4}^*=2b-2z$, $H_{2,2}=H_{3,7}=H_{5,8}=H_{9,9}=\kappa$, $H_{2,3}=-\Omega/2$, $H_{2,5}=\Omega/2$, $H_{3,1}=H_{6,3}=2\Omega$, $H_{3,3}=H_{5,5}^*=b-z+\kappa$, $H_{5,4}=H_{6,5}=-2\Omega$, $H_{6,6}=H_{6,9}=2\kappa$, $H_{7,7}=H_{8,8}^*=b-z$, $H_{9,7}=\Omega$, $H_{9,8}=-\Omega$.

In the real Gaussian field,

$$\underline{Q}_n^{(+)}=\frac{\Omega}{2}(n+1)(\underline{F}+\underline{G}) ,$$

$$\underline{Q}_n^{(-)}=-\frac{\Omega}{2}(\underline{F}+\underline{G}) ,$$

$$\mathbf{I}=-\kappa\mathbf{e}_9\delta_{n,0} ,$$

$$\underline{Q}_n=nb\underline{1}_9-\underline{L} ,$$

with $L_{1,1}=L_{4,4}^*=-2z$, $L_{2,2}=L_{3,7}=L_{5,8}=L_{9,9}=\kappa$, $L_{3,3}=L_{5,5}^*=-z+\kappa$, $L_{6,6}=L_{6,9}=2\kappa$, and $L_{7,7}=L_{8,8}^*=-z$. All other matrix elements are zero.

APPENDIX B: BROADBAND FIELDS

In this appendix we study the white-noise limit of Eqs. (15) and (26). These results shall be compared to the first-order truncation of the matrix continued fraction

$$\langle\langle x_i(t_1)x_j(t_2)\rangle\rangle=\langle\langle x_i^2\rangle\rangle\delta_{ij}e^{-b|t_2-t_1|}$$

$$\xrightarrow[b\gg\kappa,\delta,\Omega_0]{}\langle\langle x_i^2\rangle\rangle\delta_{ij}\frac{2}{b}\delta(t_2-t_1) . \quad \text{(B1)}$$

1. Cumulant expansion

For δ correlated fields, Eq. (B1), we find for the averages of

$$\frac{d}{dt}\mathbf{u}_2=[\underline{A}+x_1(t)\underline{X}_1+x_2(t)\underline{X}_2)]\mathbf{u}_2+\mathbf{I}_2\ , \tag{B2}$$

by means of the cumulant expansion [18] with $\underline{A}$ and $\underline{X}_{1,2}$ matrices, the equation

$$\frac{d}{dt}\langle\langle \mathbf{u}_2\rangle\rangle=\left[\underline{A}+\frac{\langle\langle x_1^2\rangle\rangle}{b}\underline{X}_1^2+\frac{\langle\langle x_2^2\rangle\rangle}{b}\underline{X}_2^2\right]\langle\langle \mathbf{u}_2\rangle\rangle+\mathbf{I}_2\ . \tag{B3}$$

Application of Eq. (B3) to the chaotic field gives with

$$\underline{X}_1=i\frac{\Omega_0}{2(\langle\langle \epsilon\epsilon^*\rangle\rangle)^{1/2}}(\underline{\bar{B}}+\underline{\bar{C}}),\quad \langle\langle x_1^2\rangle\rangle=\frac{\langle\langle \epsilon\epsilon^*\rangle\rangle}{2},$$

$$\underline{X}_2=-\frac{\Omega_0}{2(\langle\langle \epsilon\epsilon^*\rangle\rangle)^{1/2}}(\underline{\bar{B}}-\underline{\bar{C}}),\quad \langle\langle x_2^2\rangle\rangle=\frac{\langle\langle \epsilon\epsilon^*\rangle\rangle}{2},$$

the equation of motion

$$\frac{d}{dt}\langle\langle \mathbf{u}_2\rangle\rangle=\left[\underline{A}-\frac{\Omega_0^2}{4b}(\underline{\bar{B}}\,\underline{\bar{C}}+\underline{\bar{C}}\,\underline{\bar{B}})\right]\langle\langle \mathbf{u}_2\rangle\rangle+\mathbf{I}_2\ . \tag{B4}$$

Introducing a saturation parameter $S=\Omega^2/(b\kappa)$ we write the stationary solution of Eq. (B4) as

$$\langle\langle w\rangle\rangle=-\frac{1}{1+S},\quad \langle\langle w^2\rangle\rangle=\frac{1}{1+2S}\ . \tag{B5}$$

Note that these expressions are independent of the detuning.

For the real Gaussian field, comparing Eq. (B3) with Eq. (15) yields

$$\underline{X}_1=i\frac{\Omega_0}{2(\langle\langle \epsilon^2\rangle\rangle)^{1/2}}\underline{\bar{B}},\quad \langle\langle x_1^2\rangle\rangle=\langle\langle \epsilon^2\rangle\rangle,$$

$$\underline{X}_2=0,\quad \langle\langle x_2^2\rangle\rangle=0,$$

and

$$\langle\langle \mathbf{u}_2\rangle\rangle=-\left[\underline{A}-\frac{\Omega_0^2}{4b}\underline{\bar{B}}^2\right]^{-1}\mathbf{I}_2\ . \tag{B6}$$

We find for $\langle\langle w\rangle\rangle$ and $\langle\langle w^2\rangle\rangle$

$$\langle\langle w\rangle\rangle=-\frac{1}{1+s},\quad \langle\langle w^2\rangle\rangle=\frac{1}{1+2s-\dfrac{s^2}{1+2s+4\delta^2/\kappa^2}}\ . \tag{B7}$$

Note that the variance now exhibits a narrow resonance with width $\kappa/2$ ($S<1$).

2. Low-order truncation of the matrix continued fraction

For rapid fluctuations of the driving fields it is sufficient to retain only the first terms of the matrix continued fraction,

$$\langle\langle \mathbf{u}_2\rangle\rangle\approx[\underline{Q}_0-\underline{Q}_0^{(+)}(\underline{Q}_1)^{-1}\underline{Q}_1^{(-)}]^{-1}\mathbf{I}_2\ . \tag{B8}$$

To obtain a first approximation for a chaotic field it is permissible to neglect the second term in the denominator (because the Taylor series in the derivation had to be more specified). Inverting $\underline{Q}_0$ results in

$$\langle\langle w\rangle\rangle=\frac{1}{1+\dfrac{\Omega_0^2}{2\kappa}\left[\dfrac{1}{l_1}+\dfrac{1}{l_1^*}\right]}\ ,$$

$$\langle\langle w^2\rangle\rangle=-\langle\langle w\rangle\rangle\left[1-\frac{\Omega_0^2}{\kappa}\frac{\alpha^*\Gamma+\alpha\Gamma^*}{\alpha^*\beta+\alpha\beta^*}\right]\ , \tag{B9}$$

$$l_1=b+i\delta+\frac{\kappa}{2},\quad \Gamma=1+\frac{\kappa}{l_1}\ ,$$

$$\alpha=l_1+\kappa+\frac{\Omega_0^2}{b+i\delta+\dfrac{\kappa}{2}},\quad \beta=\alpha+2\frac{\Omega_0^2}{\kappa}\ .$$

Inspection shows that the corresponding expressions for the discussed approximations are identical with respect to lowest-order expansion.

For a real Gaussian field, there is no conceptual difference from the case discussed above, except that we have to use the continued fraction up to second order

$$\langle\langle \mathbf{u}_2\rangle\rangle=[\underline{Q}_0-\underline{Q}_0^{(+)}(\underline{Q}_1)^{-1}\underline{Q}_1^{(-)}]^{-1}\mathbf{I}_2\ , \tag{B10}$$

which results in identical expressions for $\langle\langle w\rangle\rangle$ and $\langle\langle w^2\rangle\rangle$ as in Eq. (B9). There is only a slight change within the definitions of α,β,

$$l_1=b+i\delta+\frac{\kappa}{2},\quad \Gamma=1+\frac{\kappa}{l_1},$$

$$\alpha=l_1+\kappa+\frac{\Omega_0^2}{2(i\delta+\kappa/2)},\quad \beta=\alpha+2\frac{\Omega_0^2}{\kappa}\ .$$

APPENDIX C: SLOWLY FLUCTUATING DRIVING FIELDS

If b is the smallest frequency appearing in the problem ($b\ll\kappa,\delta,\Omega_0$), we can assume that the atomic variables, which obey an equation of motion

$$\frac{d}{dt}\mathbf{u}(t)=\underline{A}(\epsilon(t))\mathbf{u}+\mathbf{I}\ , \tag{C1}$$

reach a stationary state before the field has changed significantly,

$$\mathbf{u}_s(\epsilon(t))=-\underline{A}^{-1}(\epsilon(t))\mathbf{I}\ . \tag{C2}$$

Thus it is justified to approximate the stochastic average by

$$\langle\langle \mathbf{u}(\epsilon(t))\rangle\rangle=\int P(\epsilon)\mathbf{u}_s(\epsilon)d\epsilon\ .$$

For the real Gaussian field [Eq. (13)], we find in this way

$$\langle\langle w(\epsilon)\rangle\rangle^{b=0}=\sqrt{\pi}xe^{x^2}(\mathrm{erf}(x)-1)\ ,$$

$$\langle\langle w(\epsilon)^2\rangle\rangle^{b=0}=-\langle\langle \omega(\epsilon)\rangle\rangle^{b=0}(\tfrac{1}{2}-x^2)+x^2\ ,$$

$$x=\left[\frac{(\kappa/2)^2+\delta^2}{\Omega_0^2}\right]^{1/2},\quad \mathrm{erf}(x)=\frac{2}{\sqrt{\pi}}\int_0^x e^{-x^2}dx\ . \tag{C3}$$

Far off resonance, this reduces to

$$\lim_{\delta\to\infty}\frac{\Delta[\rho_{11}(\epsilon)^{b=0}]}{\langle\langle\rho_{11}(\epsilon)\rangle\rangle^{b=0}}=\sqrt{2}\ .$$

In the same way we find for the complex Gaussian field

$$\langle\langle w(\epsilon)\rangle\rangle^{b=0}=2x^2e^{2x^2}\mathrm{Ei}(-2x^2)\ ,$$

$$\langle\langle [w(\epsilon)^2]\rangle\rangle^{b=0}=2x^2[\langle\langle w(\epsilon)\rangle\rangle^{b=0}+1]\ , \tag{C4}$$

$$x=\left[\frac{(\frac{\kappa}{2})^2+\delta^2}{\Omega_0^2}\right]^{1/2},\quad \mathrm{Ei}(a)=\int_{-\infty}^{a}\frac{e^t}{t}dt\ ,$$

and again for large detuning [compare Eq. (11)]

$$\lim_{\delta\to\infty}\frac{\Delta[\rho_{11}(\epsilon)^{b=0}]}{\langle\langle\rho_{11}(\epsilon)\rangle\rangle^{b=0}}=1\ . \tag{C5}$$

[1] Th. Haslwanter, H. Ritsch, J. Cooper, and P. Zoller, Phys. Rev. A **38**, 5652 (1988).

[2] H. Ritsch, P. Zoller, and J. Cooper, Phys. Rev. A **41**, 2653 (1990).

[3] G. Vemuri and G. S. Agarwal, Phys. Rev. A **42**, 1687 (1990).

[4] K. Rzążewski, B. Stone, and M. Wilkens, Phys. Rev. A **40**, 2788 (1989).

[5] K. Wódkiewicz, Kvant. Elektron. (Moscow) **9**, 1138 (1982) [Sov. J. Quantum Electron. **12**, 656 (1982)].

[6] M. H. Anderson, R. D. Jones, J. Cooper, S. J. Smith, D. S. Elliott, H. Ritsch, and P. Zoller, Phys. Rev. Lett. **64**, 1346 (1990).

[7] D. S. Elliott and S. J. Smith, J. Opt. Soc. Am. B **5**, 1927 (1988).

[8] M. H. Anderson, R. D. Jones, J. Cooper, S. J. Smith, D. S. Elliott, H. Ritsch, and P. Zoller, Phys. Rev. A **42**, 6690 (1990).

[9] C. Xie, G. Klimeck, and D. S. Elliott, Phys. Rev. A **41**, 6376 (1990).

[10] R. J. Glauber, Phys. Rev. **130**, 2529 (1963).

[11] B. W. Shore, *The Theory of Coherent Atomic Excitation* (Wiley-Interscience, New York, 1990), Vols. 1 and 2.

[12] A. T. Georges, Phys. Rev. A **21**, 2034 (1980).

[13] P. Zoller, Phys. Rev. A **20**, 2420 (1979).

[14] P. Zoller, G. Alber, and R. Salvador, Phys. Rev. A **24**, 398 (1981).

[15] H. Risken, *The Fokker-Planck Equation* (Springer, Berlin, 1984).

[16] R. E. Ryan and T. H. Bergeman, Phys. Rev. A **43**, 6142 (1991).

[17] C. W. Gardiner, *Handbook of Stochastic Methods* (Springer, Berlin, 1990).

[18] N. G. Van Kampen, Physica **74**, 215 (1974).